Positive Photopion Production from Hydrogen Near Threshold*

DONALD A. McPHERSON,† DUANE C. GATES,‡ ROBERT W. KENNEY, AND WILLIAM P. SWANSON§

Lawrence Radiation Laboratory, University of California, Berkeley, California

(Received 27 July 1964)

Differential cross sections for photopion production from protons were measured for 32 photon energies from 154 to 185 MeV with the Alvarez 4-in. liquid-hydrogen bubble chamber in the bremsstrahlung beam of the Berkeley electron synchrotron. High photon intensities of 1.5×10^7 MeV/pulse were used by collimating the beam down to a narrow "ribbon" which was viewed edge on by the camera. Although the pion origins were obscured by the heavy electron background, the remainder of the π track was visible for most events. Of 5000 $\pi - \mu$ decays seen, 3400 were deemed suitable for calculations. The results are in excellent agreement with the theoretical calculations by Ball, who applied the Mandelstam representation to the process. The measured values of the square of the matrix element, averaged over c.m. angles, are:

Photon energy (MeV)	154	156	160	165	170	175	180
μb/sr	16.6±4.8	15.1±0.8	14.3±0.4	15.5±0.5	16.2±0.7	16.3±1.0	12.9±1.2

All data are subject to an additional correlated error of 4.1% because of the uncertainty in the beam normalization. The cross section for the process is the product of the square of the matrix element times the kinematic factor p^*/k^*, where p^* and k^* are the c.m. momenta of the pion and the photon. Also a value of $\Lambda = (+0.931 \pm 0.59)e$ was obtained, where Λ is the multiplicative factor associated with the matrix element for photopion production from pions as calculated by Wong.

I. INTRODUCTION

THE theory of photopion production involves the least uncertainty at energies near threshold, where comparisons of theory and experiment involve the interactions in a relatively simple way. There is an intimate connection between threshold photopion production and other experimental quantities of the low-energy pion-nucleon system which have become known quite accurately in recent years.[1] These phenomena form a closed system that gives some hope of "complete" understanding if enough attention is directed toward the outstanding problems. The topic has become even more interesting since realization of the possibility of detecting contributions from the two- and three-pion resonances, and determination of new coupling constants.

Current theoretical work in photopion production is based upon dispersion relations. A series of papers is discussed to summarize the progress of this theory.[1–6] In 1957, Chew and Low evaluated the photoproduction amplitude to order $1/M$ (where M = nucleon mass), assuming a nonrelativistic Yukawa interaction between the pion and nucleon and the dominance of the 3–3 resonance in final-state scattering.[1] Chew, Goldberger, Low, and Nambu (CGLN) generalized this treatment by forming Lorentz- and gauge-invariant amplitudes expressed in terms of fixed-momentum-transfer dispersion relations.[2] Finally, Ball[3] extended the CGLN formalism, using the double spectral representation of Mandelstam.

Chew and Low first calculated the amplitudes nonrelativistically by using the interaction Hamiltonian

$$H = - \int \mathbf{j} \cdot \mathbf{A} d\mathbf{r}.$$

They considered the nucleon mass heavy enough so that nucleon recoil is negligible. The current $\mathbf{j}$ is broken into a sum

$$\mathbf{j} = \mathbf{j}_\pi + \mathbf{j}_N.$$

The current $\mathbf{j}_N$ is assumed to be independent of the meson field, and gives rise to meson production only through interaction with the magnetic moment of the nucleon because there is no nucleon-recoil term. Parity and angular-momentum considerations show that this is a magnetic-dipole interaction, with the final state having orbital angular momentum $l = 1$. Part of this state has isospin $\frac{1}{2}$ and part has isospin $\frac{3}{2}$. It is assumed that the 3–3 phase shift dominates all others, so that only final-state scattering in the 3–3 state is considered.

The current $\mathbf{j}_\pi$ gives rise to the interaction between the meson cloud and the photon. Near threshold, the most important production is by electric dipole into an s-wave final state. At threshold, this is the only mechanism for production. Chew and Low were not able to evaluate secondary scattering for this amplitude because the 3–3 final state is not involved in the s-wave dipole

[1] G. F. Chew and F. E. Low, Phys. Rev. 101, 1579 (1956); see also, for example, J. Hamilton and W. S. Woolcock, Phys. Rev. 118, 291 (1960).

[2] G. F. Chew, M. L. Goldberger, F. E. Low, and Y. Nambu, Phys. Rev. 106, 1345 (1957).

[3] J. S. Ball, Phys. Rev. Letters 5, 73 (1960); and Phys. Rev. 124, 2014 (1961).

[4] C. S. Robinson, University of Illinois Report, 1959 (unpublished).

[5] M. Cini, R. Gatto, E. L. Goldwasser, and M. Ruderman, Nuovo Cimento 10, 243 (1958).

[6] S. Mandelstam, Phys. Rev. 112, 1344 (1958); 115, 1752 (1959).

term and because the other phase shifts were not well-known at this energy.

Presently, the basic theory for pion photoproduction is the dispersion-relation approach developed by CGLN.[2] They assume that microscopic causality holds for the production process, and also that unitarity of the S matrix determines the phases of the production amplitudes. To simplify the evaluation of the dispersion relations, further assumptions are made—in particular, that the $\frac{3}{2}-\frac{3}{2}$ resonance "exhausts" the dispersion integrals. The results are expressions, expanded to order $1/M$, that contain the renormalized coupling constant f^2 and the resonance energy ω_0 as parameters.

Some calculational uncertainties are encountered, particularly in the choice of the small p-wave scattering phase shifts employed.

The generalization by CGLN led to a cross section similar in appearance to that of Chew and Low, the most significant addition being an anomalous magnetic-moment electric-dipole term. The final-state scattering contributions in the s-wave electric-dipole production were still excluded.

The CGLN approach gives an amplitude for the reaction

$$\gamma + p \rightarrow \pi^+ + n \tag{1}$$

whose dominant terms near threshold are given by the expression

$$F(\gamma + p \rightarrow \pi^+ + n)$$

$$= \frac{ef}{\sqrt{2}(1+\omega/M)} \left\{ i\boldsymbol{\sigma}\cdot\boldsymbol{\varepsilon}\left[1 - \frac{g_p+g_n}{2M}\omega + \omega^2 N^{(-)}\right] \right.$$

$$\left. + 2i\left[\frac{\boldsymbol{\sigma}\cdot(\mathbf{k}-\mathbf{q})\mathbf{q}\cdot\boldsymbol{\varepsilon}}{(\mathbf{k}-\mathbf{q})^2+1}\right] + O(q) \right\}, \tag{2}$$

where e is the electronic charge, f the renormalized pion coupling constant, $\mathbf{q}$ and ω the meson c.m. momentum and total energy, M the nucleon mass, $\boldsymbol{\sigma}$ the nucleon spin operator, $\mathbf{k}$ and $\boldsymbol{\varepsilon}$ the photon c.m. momentum and polarization vector, and g_p and g_n the full proton and neutron magnetic moments. The leading term within the first brackets is a Born term that may be interpreted as arising from the requirements of gauge invariance. The second brackets contain a Born term variously known as the direct-interaction term, or retardation term, and is completely analogous in form to the expression for the ordinary photoelectric effect. Because these terms are almost classical in origin, their importance here supports confidence in these results. The second term in the first brackets is a Born term arising from the photon interaction with the nucleon magnetic moments, and $N^{(-)}$ is a term believed to be small.

The complete CGLN amplitude for reaction (1) has been evaluated. Robinson,[4] in particular, assumed $N^{(-)}$ to be zero, and the small p-wave phase shifts to be given

by effective range formulas. He tabulated his calculations for photon energies from threshold to 450 MeV. The cross sections are isotropic near threshold, as expected from the important electric dipole-s-wave terms in Eq. (2), and the matrix element squared is nearly constant, but drops slightly above threshold owing to interference of the direct interaction term[5] with the electric dipole terms.

Important corrections have been made to the CGLN formulas since the introduction of the Mandelstam two-dimensional dispersion relations.[6] These refinements involve contributions due to intermediate two- and three-pion resonances. These states, which were originally postulated in applying the Mandelstam representation to the problem of the nucleon electromagnetic form factors,[7] have since been experimentally observed as the ρ and ω mesons.[8,9]

Ball[3] has applied the Mandelstam representation to the photoproduction amplitudes, and incorporated the parameter Λ of Wong,[10] which characterizes the strength of the photon-three-pion interaction. The interaction comes about through the exchange of a ρ meson between the nucleon and incident photon. The correction to the π^+ amplitude amounts to the addition of approximately 0.037Λ to the first bracketed terms of Eq. (2). Positive photopion production is not affected by intermediate states involving the ω particle.

The treatment by Ball using double-dispersion relations resulted in essentially the same result as that obtained by CGLN, except that a term related to the photopion production from a pion was added to the amplitude.[3] Using methods characteristic of the application of the Mandelstam representation, Ball postulates that the amplitudes representing the reactions

$$\gamma + N \rightarrow N + \pi,$$
$$\gamma + \bar{N} \rightarrow \bar{N} + \pi, \tag{3}$$

and

$$\gamma + \pi \rightarrow N + \bar{N}$$

are representations of a single set of functions that can be expressed in terms of the two-dimensional Mandelstam representation. By virtue of this common representation, there are contributions to the channel $\gamma + N \rightarrow \pi + N$ from the other two channels. According to Chew, these contributions are dominated by the intermediate states of lowest energy. For instance, the reaction $\gamma + \pi \rightarrow N + \bar{N}$ is considered in the form

$$\gamma + \pi \rightarrow \pi + \pi \rightarrow N + \bar{N}, \tag{4}$$

[7] W. R. Frazer and J. R. Fulco, Phys. Rev. **117**, 1603, 1609 (1960).

[8] A. R. Erwin, R. March, W. D. Walker, and E. West, Phys. Rev. Letters **6**, 628 (1961).

[9] B. C. Maglić, L. W. Alvarez, A. H. Rosenfeld, and M. L. Stevenson, Phys. Rev. Letters **7**, 178 (1961).

[10] How-Sen Wong, Phys. Rev. Letters **5**, 70 (1960). A more detailed account is given in Lawrence Radiation Laboratory Report UCRL-9251, 1960 (unpublished).

where the π, π system is the intermediate state with the lowest energy. Wong has studied the $\gamma+\pi \to \pi+\pi$ problem and concludes that at low energy the major contribution comes from magnetic-dipole production into the state $l=1$, $I=1$, where l and I are orbital angular momentum and isotopic spin.[10] Because he had to neglect inelastic processes, Wong obtained a homogeneous integral equation for this magnetic-dipole amplitude M_1 which required him to introduce a multiplicative constant Λ. Using the pole approximation of Chew and Mandelstam, Wong expressed M_1 in "one-pole" and "two-pole" formulas. The "one-pole" formula is

$$M_1(s) = \Lambda \frac{(1+a)}{(s+a)} \frac{D_1(1)}{D_1(s)}; \quad M_1(1) \equiv \Lambda, \qquad (5)$$

where s is the center-of-mass energy, and $D_1(-a)/D_1(s)$ is the pion form factor obtained by Frazer and Fulco.[7] The parameter $(-a)$ is the location of the effective pole on the real axis, and is given by Wong as $a \approx 5.7$, $(\hbar = c = \mu = 1)$.

Frazer and Fulco have studied the remaining process, $\pi+\pi \to N+\bar{N}$. Using a one-pole approximation, they were able to express the amplitude in explicit form.

By combining these results, Ball was able to calculate the contributions from the $\gamma+\pi \to N+\bar{N}$ channel. In addition he was able to avoid the $1/M$ expansion used by CGLN; however, he did not include the secondary scattering effects in the s-wave state. If M' is the amplitude for production without the $\pi-\pi$ effect, then according to Ball the $\pi-\pi$ interaction changes $|M'|^2$ by a factor $1+(0.074\Lambda/e)$, wereh e is the electronic charge.

Ball estimated the value of $N^{(-)}$ to be 4.5×10^{-3}. His comparison with experimental data allowed values of Λ as large as ± 1.8.

Other workers have calculated the effects of an intermediate pion-pion reasonance, and compared them with data, particularly with R,[11] the ratio of negative to positive photopion production from deuterium. DeTollis et al.[12] found that $\Lambda = +0.6$ would produce satisfactory agreement with experimental values for R and for neutral pion production.

Besides the pion-pion resonance contribution, Warburton and Gourdin[13] have calculated the effect of a pion-nucleon intermediate state with $J=\frac{1}{2}$. Their results favor a value $\Lambda = +2.0$, to fit experimental values of R at higher energies, but state that the bipion and rescattering terms cancel at threshold.

Robinson et al.,[14] using calculations by McKinley,[15]

have stated that a negative value $\Lambda = -1.5 \pm 0.5$ was required to fit their higher-energy photoproduction data at backward angles. Their calculation did not include the $\frac{1}{2}$, $\frac{1}{2}$ rescattering term of Warburton and Gourdin.[13]

These results point to the conclusion that the theory including pion-pion resonances is in an unsatisfactory state at present, and the "complete" understanding hoped for until recently has not yet been realized. It appears that experimental data on reaction (1) near threshold agree with the CGLN formulas with no pion-pion resonance correction required, and that consistency with the other low-energy parameters is satisfactory.[1] The effects of corrections to the CGLN formulas have not yet been detected near the photopion threshold.

The present work was undertaken in order to test the theory by measuring more accurately the differential cross section for the reaction $\gamma+p \to \pi+n$ very near threshold. The systematic uncertainties in these observations, taken in a hydrogen bubble chamber, are quite different from those of other techniques, using counters or plates. Our measurements are reduced to the energy-dependent matrix element for the reaction under study, and a value for Λ is found.

II. EXPERIMENTAL TECHNIQUE

In this experiment 180 000 photographs were taken of interactions in the 4-in. liquid-hydrogen bubble chamber situated in the bremsstrahlung beam of the Berkeley electron synchrotron. The accelerator was operated at 189.1 MeV. Acceptable photoproduction events were restricted to photons in the interval 153 to 186 MeV.

The photon beam incident upon the bubble chamber had a thin ribbonlike rectangular cross section which was approximately uniformly intense. The camera viewed this "ribbon" beam edge-on. The beam intensity was high enough to mask a strip along the center portion of the chamber with a ribbon of bubbles created by the large number of electrons produced in the forward direction.

The beam intensity was limited to 1.5×10^7 MeV/pulse by our tolerance for electron background outside the beam volume. This intensity was, however, 15 times that used in previous bubble-chamber threshold photoproduction experiments.[16] Miller and Hill originated this technique.[17]

Figure 1 is a photograph of a $\pi-\mu$ decay in a liquid hydrogen chamber. The uncertainty in the origin of this pion is only the half-width of the beam, 0.20 cm. For a 5-MeV pion at 90 deg, this corresponds to an uncertainty of ± 0.4 MeV kinetic energy, or an uncertainty of ± 0.6 MeV in laboratory-system photon energy.

[11] See, for example, W. R. Hogg, Proc. Phys. Soc. (London) **80**, 729 (1962), for a review of data on R.

[12] B. De Tollis and A. Verganelakis, Nuovo Cimento **22**, 406 (1961); and B. De Tollis, E. Ferrari, and H. Munczek, ibid. **18**, 198 (1960).

[13] A. E. A. Warburton and M. Gourdin, Nuovo Cimento **22**, 362 (1961).

[14] C. S. Robinson, P. M. Baum, L. Criegee, and J. M. McKinley, Phys. Rev. Letters **9**, 349 (1962).

[15] J. M. McKinley, University of Illinois Technical Report No. 38, 1962 (unpublished).

[16] D. C. Gates, R. W. Kenney, D. A. McPherson, and W. P. Swanson, Rev. Sci. Instr. **31**, 565 (1960).

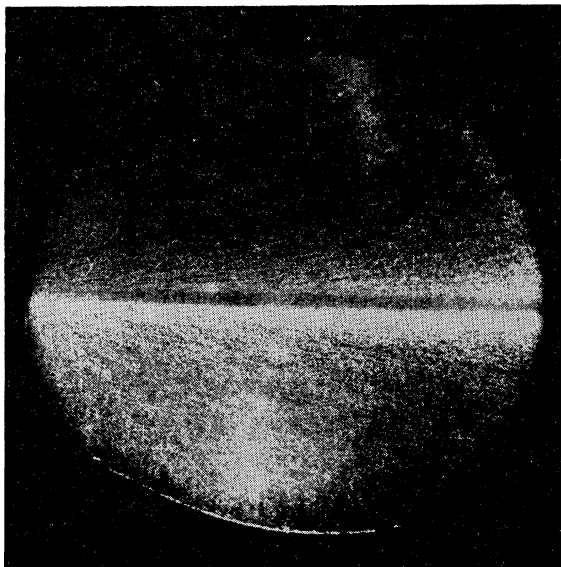[17] Donald H. Miller and D. A. Hill, private communication to Robert W. Kenney.

FIG. 1. A π-μ decay. Background is so heavy at the center that it blanks out the light and causes the dark streak at the beam region. The beam enters from the left.

Figure 2 is a schematic diagram of the experimental apparatus. The tubes of lithium hydride shown in Fig. 2 were placed in the beam to absorb selectively the very-low-energy photons which produce only electron background. Nearly all photons below 10 MeV were absorbed, whereas the transmission of photons about the threshold energy was 0.512.

The thick-wall ionization chamber shown in Fig. 2 was identical to the chamber developed at Cornell,[18] and was used as the primary monitor of the beam. The magnets between the two walls of lead shielding swept
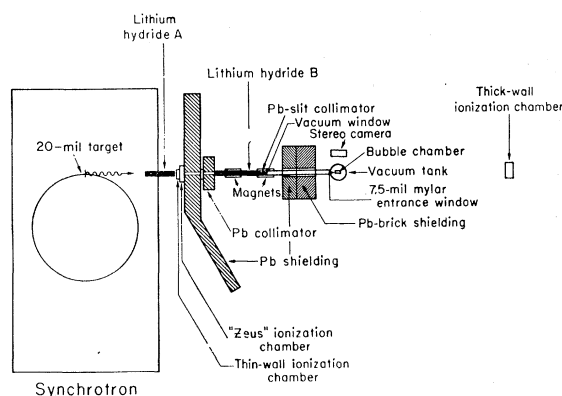

FIG. 2. Experimental setup for film taking. Beam leaves the synchrotron on the left and is "hardened" by the tubes of lithium hydride, A and B. After being collimated by the slit collimator, it enters the vacuum system of the bubble chamber. The thick-wall Cornell ionization chamber which monitored the beam is on the far right.

[18] D. R. Corson, J. W. DeWire, B. D. McDaniel, and R. R. Wilson, Office of Naval Research Report, 1953 (unpublished).

charged particles from the beam. A vacuum pipe, coupled directly to the bubble-chamber vacuum system, was extended into the final sweeping magnet so that electrons from its entrance window, as well as from the slit collimator, were also swept from the beam, allowing the pure photon beam to traverse the entrance window of the bubble chamber. The window was a 7.5-mil film of Mylar, and the electron background it produced was not obtrusive. The size of the photon beam profile in the chamber was 0.37×1.7 cm.

The chamber repetition period was 6 sec, which afforded sufficient time between pulses for stable operation. Pre-expansion temperature and pressure were 29.5°K and 115 psia. The hydrogen density was 0.0552 g/cm³. (This was determined by substituting the muon energy and average range into a range-energy relationship and solving for density.) The chamber was operated so that the ionization of single relativistic electrons gave a very low bubble density, although the more heavily ionizing pions left visible tracks.

III. SCANNING AND MEASURING

The film was scanned three times by a group of seven people using stereoscopic devices. It is obvious from Fig. 1 that scanning efficiency close to the beam was below average. However, the over-all scanning efficiency of three scans was greater than 99% in all regions of the chamber farther than 1 cm from the beam region.

The events were measured on a digitized apparatus to determine (a) range of the π, (b) angle of the π with respect to the beam θ, (c) muon range, (d) angle between the μ and the π, (e) location of the event in the chamber. Items (a) and (b) are used to calculate the kinematics of the photoproduction. Item (c) is used to determine the density of the liquid hydrogen from range-energy relations. The last two are used to calculate the probability of seeing and identifying an event. The pion kinetic energy T_π was determined from the range-energy relation,

$$\ln T_\pi = 3.056 + 0.548 \ln R_\pi; \quad R_\pi \text{ given in g/cm}^2.$$

The rms errors of the measured pion angle include multiple-scattering effects. Because of the origins of the events were obscured, there is an inherent uncertainty in a pion track length of more than one-half the width of the photon beam profile. This constitutes an error on the order of 1 MeV in photon energy. Actual measuring errors also contribute about 1 MeV error, so the energy resolution is between 1 and 2 MeV. The angular resolution in the lab frame of reference is 2 deg.

IV. PHOTON BEAM NORMALIZATION

In order to calculate the photon flux that passed through the chamber, the following parameters were required:

Peak energy, 189.1±3.7 MeV;

LiH transmission, 0.512±0.006;

LiH in-out ratio, 0.484±0.007;

Cornell chamber response, $(3.83±0.12)×10^{18}$ MeV/C.

The first two items were determined by using a pair spectrometer. The LiH transmission was constant in the photon energy interval from 150 to 185 MeV. The third item, the LiH in-out ratio, was determined by monitoring the synchrotron beam with a thin-walled ionization chamber placed in front of the LiH and by measuring the increase in the charge per unit beam collected from the Cornell chamber when the LiH was removed. The Cornell chamber response was calculated from the data of Loeffler et al.[19]

The bremsstrahlung spectrum was calculated from the bremsstrahlung cross section of Olsen and Maximon.[20,21] Multiple scattering of electrons in the target was accounted for by a method similar to that of Hisdal.[22] Other synchrotron target corrections were made according to the method of Wilson.[23] The rectangular shape of the collimator was accounted for in the calculation of the spectrum.

V. RESULTS

The differential cross section for laboratory photon energy k and c.m. pion angle θ^* is related to the number of events seen in a solid-angle interval $\Delta\Omega^*$ and energy interval Δk as follows:

$$\Delta\Omega^*\Delta k\frac{d\sigma}{d\Omega^*}\times\left(\frac{\text{protons}}{\text{cm}^2}\right)\times\mathfrak{N}(k)\times\text{Eff}(k,\theta)$$

$$=\sum_{r=1}^{5}\frac{\text{events seen in region } r \text{ in } \Delta k\Delta\Omega^*}{\text{scanning efficiency in region } r}, \quad (6)$$

where $\mathfrak{N}(k)$ is the total photon flux per MeV and $\text{Eff}(k,\theta)$ is the geometrical chamber efficiency. Notice that allowance is made for uneven scanning efficiencies by summing over various regions in the chamber.

The chamber efficiency is the ratio of the pion solid angle in the chamber in which an event could be identified to the total pion solid angle in which the event could be produced in the chamber. For this calculation the beam region is considered as though enclosed between two slightly diverging planes at an angle of 8 deg to each other. The fiducial volume excludes the wedge-shaped beam. It was required that each acceptable event have its $\pi-\mu$ vertex within the fiducial volume and have its muon positively identified.

[19] F. J. Loeffler, T. R. Palfrey, and G. W. Tautfest, Nucl. Instr. Methods 5, 50 (1959).

[20] H. Olsen and L. C. Maximon, Phys. Rev. 114, 887 (1959).

[21] H. W. Koch and J. W. Motz, Rev. Mod. Phys. 31, 929 (1959). (This is a complete review of bremsstrahlung cross sections.)

[22] E. Hisdal, Phys. Rev. 105, 1821 (1957).

[23] R. Wilson, Proc. Phys. Soc. (London) A66, 638 (1953).

An essential complication must be considered. The latitude allowed in operating temperature of the bubble chamber was approximately ±1%. If the temperature dropped more than 1%, the pions did not leave satisfactorily dense tracks, and if the temperature rose more than 1%, the background obscured a large portion of the chamber. Therefore the film was classified according to the appearance of the background near the beam. These classifications were:

Type 0. Chamber insensitive (cold).

Type 1. Obscuring background within two diverging planes 0.93 cm apart at center of chamber.

Type 2. Same as type 1 except with a 1.98-cm separation.

Type 3. Same as type 1 except with a 3.40-cm separation.

The separation for type 1 was so chosen that 155-MeV events could be included in the analysis. Type 3 was set so that there was no noticeable drop in the distribution of muon origins outside the beam region for any type of film. Type 2 was established arbitrarily at some intermediate position. Of the usable film (types 1, 2, and 3), two-thirds was of type 1, one-third was of type 2, and only a few percent was of type 3.

The film was classified on the appearance of the electron background only. To avoid bias, we scanned first for background quality at the high rate of 2 or 3 pictures per second. The $\pi-\mu$ decays were not distinguishable at that speed and presumably did not affect our judgment of the film. Whenever changes in operating conditions were observed, the film classification was changed. Any given frame was then assigned the classification of that region of the film in which it was located.

The relation of the cross section to the number of observed events must be generalized to sum over various film types i (where $i=1, 2, 3$). The geometrical chamber efficiency, $\text{Eff}(k,\theta)$, is different for each type of film, so $\text{Eff}(k,\theta) \rightarrow \text{Eff}_i(k,\theta)$. The number of photons in the energy interval Δk must be subdivided into the number that traversed the chamber for pictures of type i. The final expression for calculation is then

$$\frac{d\sigma}{d\Omega^*}=\frac{\sum_{r=1}^{5}\dfrac{\text{events seen in region } r \text{ in } \Delta\Omega^*\Delta k}{\text{scanning efficiency in region } r}}{\left(\dfrac{\text{protons}}{\text{cm}^2}\right)\times\sum_{i=1}^{3}\mathfrak{N}_i(k)\times\text{Eff}_i(k,\theta)\times\Delta\Omega^*\Delta k}. \quad (7)$$

About 3400 $\pi-\mu$ decays were observed within the fiducial volume of the chamber and also within the angular range that was free from systematic observational errors.

For the data from 161 to 185 MeV, the angular regions in which the data were considered free of systematic error were chosen by considering the geometrical effi-
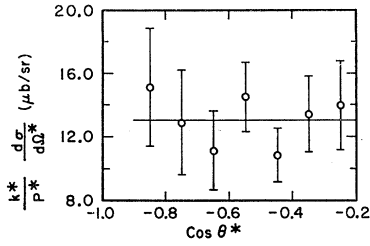
FIG. 3. Typical angular distribution for the matrix element squared. These data are for photopions produced by 164-MeV photons. The forward hemisphere is included in data for other energies. Errors are counting errors only.

ciencies for each photon energy and accepting only that range of c.m. angles in which efficiencies were greater than one-half the maximum value.

For energies from 154 to 160 MeV the limits were chosen wherever the actual pion distribution or the distribution predicted by geometrical efficiency fell off by a factor of 2 from the maximum. Of the 4400 available events, 3400 were within these angular limits and were usable for further calculations.

Figure 3 is the angular distribution at 164 MeV. The ordinate is the differential cross section multiplied by the kinematic factor k^*/p^*, where k^* and p^* are the c.m. photon and pion momenta. Figure 3 is typical of the angular distribution and is consistent with an isotropic distribution in the center of mass. Experimental data[24–27] at $k=185$ MeV show essentially no $\cos\theta$ component. Our data, taken nearer threshold, are not expected to show p wave properties, particularly in view of their statistical accuracy.

In the appropriate averaging process over pion angles, Eq. (7) becomes

$$\left\langle \frac{d\sigma}{d\Omega^*} \right\rangle = \frac{\sum\limits_{r=1}^{5} \dfrac{n(k,r)}{\text{scan efficiency in region } r}}{(\text{protons/cm}^2)\sum\limits_{i=1}^{3} \mathfrak{N}_i(k)\Delta k \displaystyle\int \text{Eff}_i(k,\theta)d\Omega^*}, \quad (8)$$

where i is the film classification, r is the scanning region, and $n(k,r)$ is the number of events in region r within the acceptable angular range, produced by photons in the energy range Δk.

The results are listed in Table I and are plotted in Fig. 4, which shows the average matrix element squared

[24] M. I. Adamovich, E. G. Gorzhevskaya, V. G. Larionova, V. M. Popova, S. P. Kharlamov, and F. R. Yagudina, Zh. Eksperim. i Teor. Fiz. 38, 1078 (1960) [English transl.: Soviet Phys.—JETP 11, 779 (1960)].
[25] G. M. Lewis and R. E. Azuma, Proc. Phys. Soc. (London) A73, 873 (1959).
[26] A. Barbaro, E. L. Goldwasser, and D. Carlson-Lee, Bull. Am. Phys. Soc. 4, 23 (1959).
[27] M. Beneventano, G. Bernardini, D. Carlson-Lee, G. Stoppini, and L. Tau, Nuovo Cimento 4, 920 (1956).

versus lab photon energy. As before, the ordinates are the actual cross sections multiplied by the kinematic factor k^*/p^*. The solid line in Fig. 4 is the theoretical cross section calculated by Ball with $\Lambda=0$. The two dashed lines represent the cross section with $\Lambda=\pm1.8e$, which are considered to be the largest reasonable limits for Λ, consistent with the experiment. Previous experimental points are included as noted on the figure.

The standard deviations quoted in Table I and Figs. 3 and 4 are counting errors only. In addition, there is a correlated beam normalization error. In Sec. IV, four parameters were used to normalize the beam. The errors on these parameters constitute a relative error of 4.1% for all cross sections. This normalization error was not included in Fig. 4 because it is a scale factor that does not affect the relative energy distribution of the events.

We fit the theory to the data by adjusting the value of the parameter Λ. This parameter (discussed in Sec. I) is the multiplicative constant of the matrix element for pion photoproduction from a pion into a final state of angular momentum $l=1$.

The Λ fitting procedure must be compatible with the statistical distribution of the data. First we write the form

$$\frac{k^*}{p^*}\frac{d\sigma}{d\Omega^*}=|M_k|^2=\frac{N_k}{W_k}; \quad k=154, \cdots, 185. \quad (9)$$

The numerator N_k is the sum of all events in the energy interval $k\pm\frac{1}{2}$ MeV (actually the sum of the inverses of the scanning efficiency for each event), and the denominator W_k is the appropriate weighting factor. The product $|M_k|^2W_k$ is Poisson-distributed, so the probability for measuring some particular $|M_k|^2$ is given by

$$P(|M_k|^2W_k)=\frac{(|M_k|^2W_k)^{N_k}}{N_k!}\exp(-|M_k|^2W_k). \quad (10)$$

From Sec. I we have

$$|M_k|^2=\left(1+\frac{0.074\Lambda}{e}\right)|M_k'|^2, \quad (11)$$

where the matrix element $|M_k'|^2$ for the photopion production without a bipion correction is given by

TABLE I. Matrix element squared, averaged over center-of-mass angles.

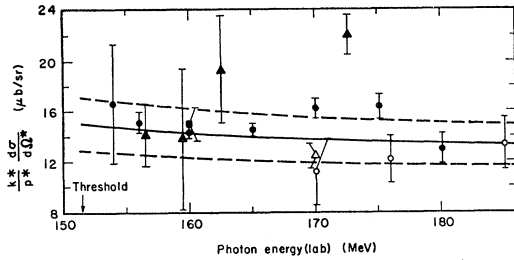| k_{lab} (MeV)	M^2 (μb/sr)
154	16.6±4.8
156	15.1±0.8
160	14.3±0.4
165	15.5±0.5
170	16.2±0.7
175	16.3±1.0
180	12.9±1.2

FIG. 4. Matrix element squared, averaged over c.m. angles, as a function of laboratory photon energy. Errors are counting errors only and all data are subject to correlated normalization error of 4.1%. ● This experiment. ▲ Adamovich *et al.* (Ref. 24). ○ Lewis and Azuma (Ref. 25). ■ Barbaro *et al.* (Ref. 26). △ Beneventano *et al.* (Ref. 27). The solid line is Ball's result for $\Lambda=0$. The two dashed lines give his results for $\Lambda=\pm1.8e$; the upper curve is for $\Lambda=+1.8e$.

Ball. Using the $|M_k'|^2$ and knowing the probability $P(|M_k|^2W_k)$ we can calculate the most probable Λ from

$$1.0+\frac{0.074\Lambda}{e}=\frac{\sum_k N_k}{\sum_k |M_k'|^2 W_k}=1.0689, \qquad (12)$$

which gives $\Lambda\approx0.931$. The sum over k is the sum over all energy bins.

The effect of the counting statistics on the error in Λ is negligible, since 3351 events were used. The absolute error on $1+0.074\Lambda/e$ is the relative normalization error (4.1%, given above). Thus the error on Λ is due to the normalization error only, and we have

$$\Lambda=(+0.931\pm0.59)e.$$

Further improvement in beam calibration techniques will permit the error on Λ to be decreased. Ball notes

that the value of Λ is also affected by error in the pion-nucleon coupling constant $f^2=0.08$, which he used in calculating the theoretical cross section.

VI. CONCLUSIONS

The measured angular distributions are consistent with isotropy within angular ranges of the acceptable data. This agrees with the prediction that near threshold the process is primarily electric-dipole into a final s-wave state.

Table I shows the squares of the matrix element averaged over the c.m. angle of the pion. These data, which are plotted in Fig. 4, show that the variation with photon energy and the magnitudes of the matrix element squared are in general agreement with the theoretical calculations by Ball, although there is scatter in the data. In addition, there is good agreement with the previous experimental data, except for the 172.5-MeV point of Adamovich *et al.*[24]

Finally, the value obtained for the parameter Λ shows that the effect of the $\pi+\gamma\rightarrow N+\bar{N}$ channel on the reaction studied here is small.
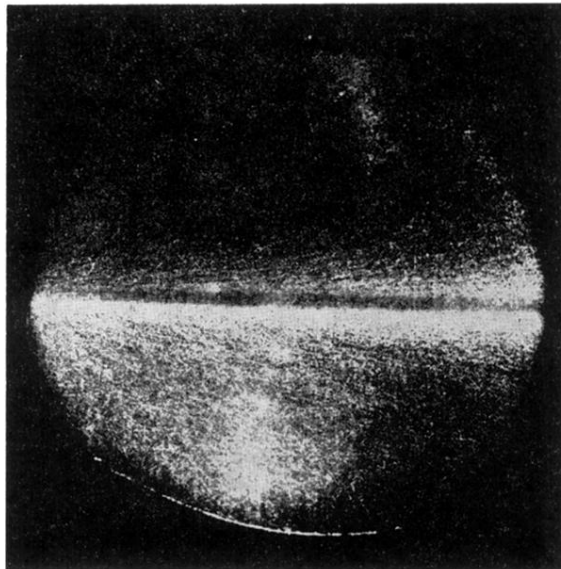
FIG. 1. A π-μ decay. Background is so heavy at the center that it blanks out the light and causes the dark streak at the beam region. The beam enters from the left.